

# 3D Printed Liquid Jet Impingement Cooler: Demonstration, Opportunities and Challenges

T.-W. Wei<sup>1,2</sup>, H. Oprins<sup>1</sup>, V. Cherman<sup>1</sup>, I. De Wolf<sup>1,3</sup>, E. Beyne<sup>1</sup>, S. Yang<sup>2,\*</sup>, M. Baelmans<sup>2</sup>  
<sup>1</sup>imec, Leuven, Belgium, <sup>2</sup>Dept. Mech. Eng. KU Leuven, Leuven, Belgium, <sup>\*</sup>Member of Flanders Make  
<sup>3</sup> Dept. Materials Eng. KU Leuven, Leuven, Belgium  
 email: [tiwei.wei@imec.be](mailto:tiwei.wei@imec.be)

**Abstract**—Liquid jet impingement cooling is a very efficient cooling technology for high performance devices. Previous studies demonstrated that polymers can be used as a cost effective alternative for Si for the fabrication of impingement coolers. The recent developments in additive manufacturing or 3D printing technology enable the potential to fabricate low cost polymer coolers with complex internal channels. In this paper, the use of 3D printing is discussed for the fabrication of a chip level polymer impingement cooler. The paper presents the cooler design, the manufacturability aspects and the characterization of several 3D printed coolers with different nozzles arrays. The challenges and opportunities for the use of 3D printing for this applications are discussed. A methodology to provide design guidelines for 3D printed liquid impingement jet coolers is elaborated.

**Keywords**—component; 3D printing; impingement jet cooling; challenges; design guidelines

## I. INTRODUCTION

Thermal management of high performance electronic applications becomes more and more challenging, especially for three-dimensional (3D) chip stacks [1]. Liquid jet impingement cooling with a locally distributed return network is regarded as an efficient way to cool down the chip temperature [2]. In order to be compatible with the chip packaging process flow, different fabrication techniques were investigated to build chip level cooler with micron-size jet arrays, such as Si DRIE microfabrication [3], multilayer ceramic technology (MLC) [4] and lithography electroforming micro molding (LIGA) [5]. However, these techniques are all very expensive. We previously demonstrated that cost efficient mechanical micro-machining techniques could be used to fabricate a polymer chip level 3D-shaped cooler with sub-mm nozzle diameters with a very good thermal performance [2]. The mechanical machining process has however limitations to further scale down the nozzle diameters in order to obtain better thermal performance. Moreover, different internal structure layers have to be fabricated separately and subsequently assembled. Due to the recent developments in additive manufacturing or 3D printing, its fabrication capabilities are reaching the required dimensions for electronic packaging. Therefore, 3D printing or additive manufacturing is generating a lot of attention in the packaging community for applications such as MEMS packaging [6], transmission lines [7], antennas [8], and fan-out wafer level packaging (FOWLP) [9,10]. Due to the advantages of low cost fabrication and the capability to create complex geometries, 3D printing has the potential to

be used to fabricate cost efficient polymer impingement coolers. Furthermore, it allows to print the whole structure in one part and to customize the cooler design to match the jet nozzle array to the chip power map. However, currently there are several limitations for the 3D printing technology to build structurally sound sub-mm structure, especially for polymer based structures.

In this work, we will first discuss the cooler design in terms of the nozzle array and diameters and the plenum height. Moreover, the impact of the material properties on the heat transfer is illustrated. In the next section, an overview of the state of the art for the relevant 3D printing technologies for this kind of application is given. Next, the quality of the printed structures and their thermal performance is evaluated for different cooler designs. Furthermore, measurement methodologies are introduced for the assessment of the fabrication tolerance and for defect inspection. Finally, the challenges and opportunities for the use of 3D printing for the fabrication of coolers are discussed. The objective of this work is to provide a guideline for the 3D printed micro-jet cooler design and fabrication, including materials selection, plenum thickness design, critical nozzle diameters design and structural integrity.

## II. JET IMPINGEMENT COOLER DESIGN

Conventional liquid cooling solutions have two major thermal bottlenecks: the presence of the thermal interface material (TIM) and the lateral temperature gradient across the chip surface. Jet impingement cooling with locally distributed outlets has the advantages to overcome these problems since the liquid coolant is directly ejected from nozzles on the chip backside resulting in a high cooling efficiency. Moreover, it can also enable hot spot targeted cooling with a customized design of the nozzle array. The schematic of the cooler with distributed inlets and outlets is shown in Fig.1 (a). The internal structure includes inlet/outlet tubes for connections, an inlet plenum for feeding the liquid into individual inlet nozzles, and also the outlet plenum for collecting the outflow. The distributed inlets and outlets in the nozzle plate form the nozzle array, for which a top view is shown in Fig.1 (b). The cavity height of the structure is defined as the distance between the nozzle plate and the chip backside which is cooled by the coolant. The interactions between inlet flows and outlet flows happen in this region. For the modeling methodology, conjugate heat transfer and fluid dynamics simulations are used in the Computational fluid dynamics (CFD) models to assess the thermal and

fluidic behavior of the cooler. First, a unit cell simulation is created to study the thermal and hydraulic performance of the cooler for different geometries of the nozzle array. Next, a plenum level model and a full cooler model are used to study the interaction between inlet plenum thickness and nozzle diameter, as well as the impact of the thermal conductivity of the cooler material. In this section, the results of the modeling study, the required trends for thermal performance improvement and the link with the fabrication tolerances are discussed.

The considered chip size in this work is  $8 \times 8 \text{ mm}^2$  with 0.2 mm thickness. The distance between the jet nozzles and chip cooling surface is fixed at 0.2 mm. For the cooler optimization, the flow rate for all cooler designs is kept equal to 530 mL/min. The inlet temperature is set at  $10^\circ\text{C}$ . The chip power is 24 W. The nozzle numbers are ranging from  $N=1$  to  $N=32$ . The dimensionless inlet diameter  $d_i/L$  ranges from 0.025 to 0.4.

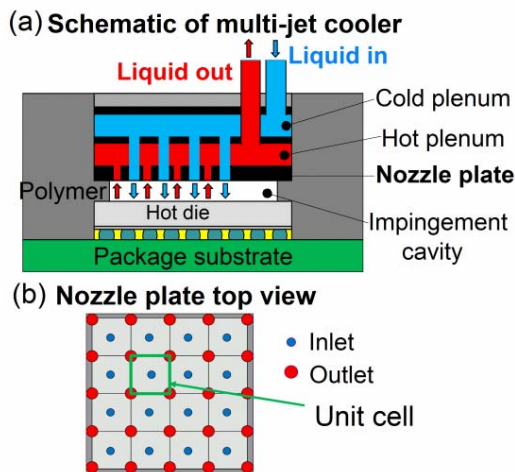


Figure 1. Schematic of impingement jet cooler. *A*: Cross-section of the chip level jet impingement cooler revealing the internal structure with inlet and outlet plenum, the nozzle plate and the impingement cavity. *B*: Top view of the distribution of the inlet and outlets in the nozzle plate.

#### A. Nozzle array scaling analysis

Since the nozzle arrays present quasiperiodic behavior (Fig.1(b)), a unit cell CFD model can be used to analyze the thermal and fluidic behavior. For each unit cell, one inlet nozzle is shared by 4 four outlets. In order to optimize the performance of the jet impingement cooler the following five design parameters need to be considered: nozzle number  $N$ , inlet diameter  $d_i$ , outlet diameter  $d_o$ , nozzle thickness  $t$  and cavity height  $H$ . In addition, fluid dynamics parameters such as flow rate, pressure drop and pump power need to be optimized. From the heat transfer and fluid dynamics theory, the dimensionless analysis is known as a very powerful tool to design the experiments. It specifies that the physical behavior of the impingement cooler is determined by the proportions of the geometrical design parameters (the dimensionless parameters) and is applicable for an arbitrary absolute dimensions. This phenomenon can be exploited to generalize the obtained modeling results and to understand the scaling trend of the number of nozzles in the array and of

the jet diameters for the multi-jet impingement cooler. Using this approach, the problem of design optimization where five independent design parameters introduced above need to be considered, can be generalized by replacing these parameters with four dimensionless variables:  $d_i/L$ ,  $d_o/L$ ,  $H/L$  and  $t/L$ , where  $L=D/N$  and  $D$  is the size of the chip to be cooled.

In order to evaluate the performance of the jet impingement cooler, the thermal resistance and pumping power are both considered for the optimization. In the previous study [2], we illustrated the trade-off between thermal resistance and pump power: the thermal resistance can be further reduced by increasing the flow rate, however at the expense of the required pump power. In this work, the impact of the cooler geometry on the two objective values (thermal resistance and pump power) is studied systematically.

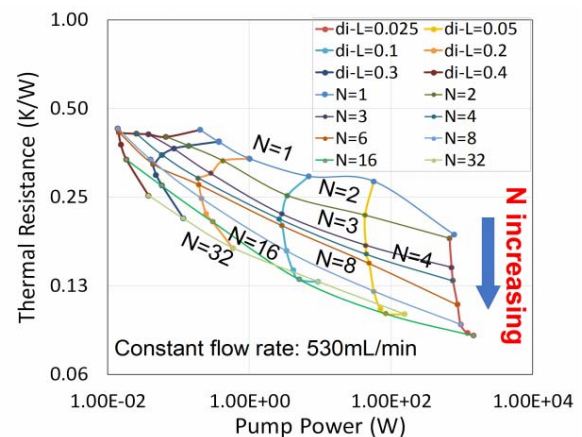


Figure 2. Results of the unit cell CFD simulation: Average thermal resistance as function of pumping power for the different nozzle diameter ratios and number of nozzles.

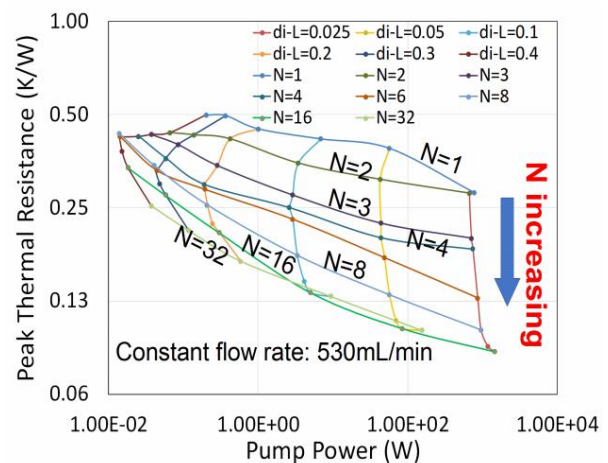


Figure 3. Results of the unit cell CFD simulation: Maximal thermal resistance as function of pumping power for the different nozzle diameter ratios and number of nozzles.

Fig.2 and Fig.3 show the visual representation of the trade-off between the obtained thermal resistance and the required pumping power for the average and maximum temperatures respectively. For the best thermal performance

both the thermal resistance as well as the pumping power should be as low as possible. This can therefore be considered as a multi-objective optimization [11]. The figures show that with the same nozzle number  $N$ , the thermal performance improves as the inlet diameter ratio  $d_i/L$  decreases. On the other hand, the pumping power increases for smaller  $d_i/L$  ratios, making this less energy efficient. From the two figures with average temperature and peak temperature, we can see that a nozzle array with higher nozzle number  $N$  can achieve lower thermal resistance and lower pumping power. However, the performance will saturate beyond a certain number, under the assumption of a fixed cavity height. In the considered case, the diameter of the nozzles for such a ‘saturated’ thermal performance is in the order of 100  $\mu\text{m}$ .

### B. Plenum level modeling

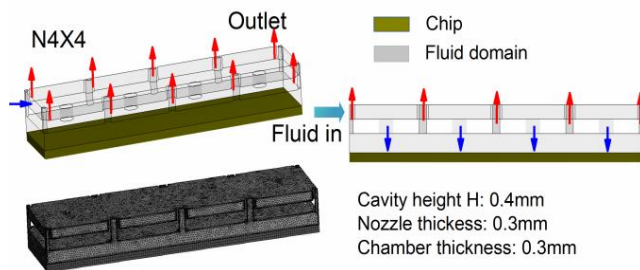


Figure 4. Schematic and grid of the conjugated CFD model for the plenum level study for 4 inlet nozzles.

(1) *Lateral feeding plenum*: A temperature gradient across the chip surface due to non-uniform cooling can reduce the cooling efficiency. In order to reduce the temperature gradient across the chip surface, the flow distributions should be uniform when the inlet flow comes from the inlet plenum. Therefore, the plenum level modeling is very important for the cooler design. In this paper, two different kinds of plenum feeding methods are studied: the inlet flow coming from one side and the inlet flow coming from the top plenum. Fig. 4 shows the plenum level CFD model that is used to study the interaction between several nozzles and between the nozzles and the plenum. The nozzle array is chosen as 4×4. The boundary conditions applied on the two sidewalls are periodic.

As shown in Fig.4, the flow is assumed to come from the left opening channel. The boundary condition of the inlet is based on velocity while the outlet pressure is fixed. The cavity height (nozzle-to-target distance) is set to 0.4 mm, and the nozzle plate thickness amounts to 0.3 mm. The inlet plenum chamber thickness is 0.3 mm. The objective of this DOE is to study the impact of the nozzle diameter on flow distributions and temperature uniformity. With other parameters kept constant, the inlet diameters are increasing from 0.2 mm to 1 mm. From the flow field distribution shown in Fig.5 it is seen that, the flow distributes uniformly along the channel when the inlet nozzles are smaller. As the inlet nozzle becomes larger, the flow will mostly go through the inlet nozzles near the entrance and decay along the flow

direction. Moreover, recirculation flow will occur when the nozzle diameter is larger.

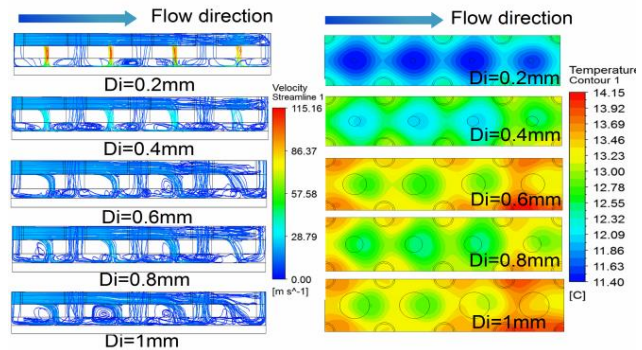


Figure 5. Modeling results from the plenum level model: impact of inlet nozzle diameter on the chip uniformity.

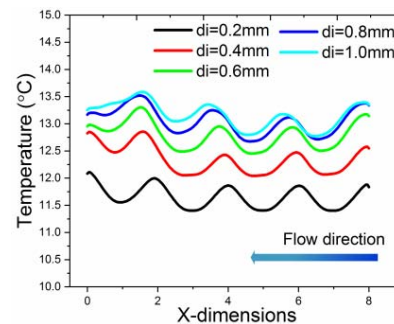


Figure 6. Modeling results from the plenum level model: chip temperature profile for different inlet diameters.

As shown in Fig.6, it can be seen that smaller diameter can achieve more uniform temperature distribution and lower temperature. The reason is that the inlet nozzle velocity becomes larger as the inlet diameter is smaller when the total inlet flow rate is kept constant.

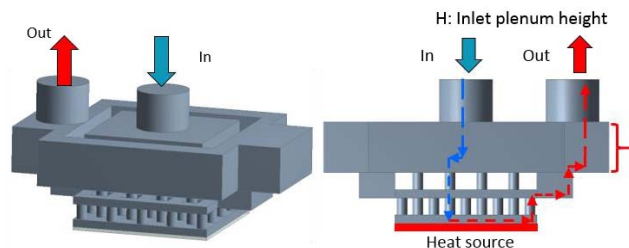


Figure 7. CFD model of the full impingement cooler. Only the fluidic domain is visualized.

(2) *Central feeding plenum*: In order to study the inlet flow rate distribution with regards to different inlet plenum heights, a CFD model of the full cooler, shown in Fig.7, is used. This allows to simulate the flow interactions and flow rate distribution patterns. The inlet flow comes directly from the top plenum and the inlet tube is located above the center of the nozzle array. Moreover, complex flow phenomenon can be visualized through the flow streamlines. However, this type of simulation is very time consuming. As shown in Fig.8, a lower plenum height can generate more flow maldistributions, with higher velocity concentrating in the

nozzles in the center of the cooler. This indicates that it is important to balance the inlet diameter and plenum height when designing the impingement cooler.

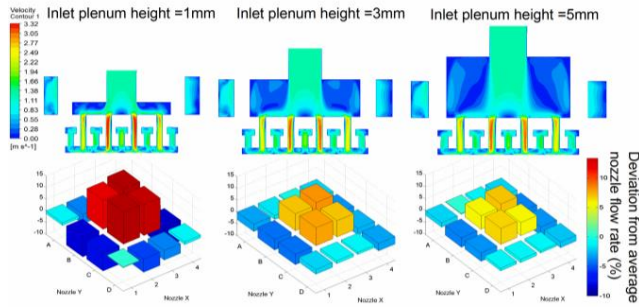


Figure 8. Impact of the plenum level thickness on the flow distribution in the 4x4 array of inlet nozzles.

### C. Influence of cooler materials

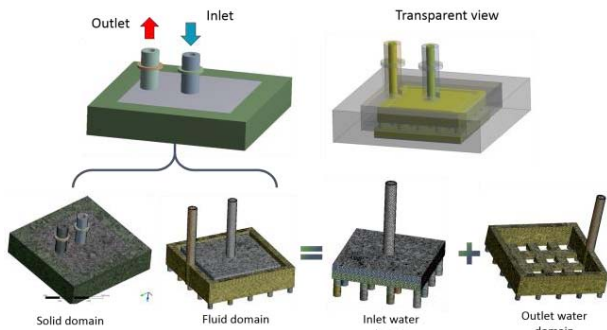


Figure 9. CFD model of 3D printed cooler with solid and fluid domains.

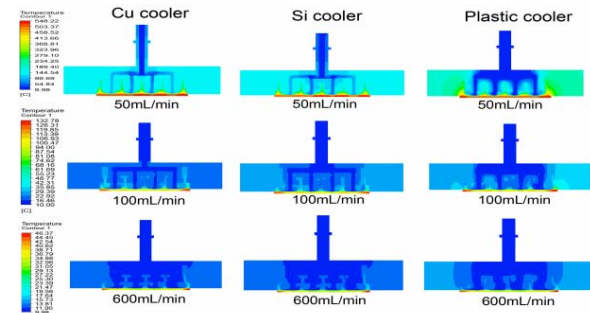


Figure 10. Contour plots of the full cooler CFD models showing the impact of the thermal conductivity of the cooler materials for different flow rates.

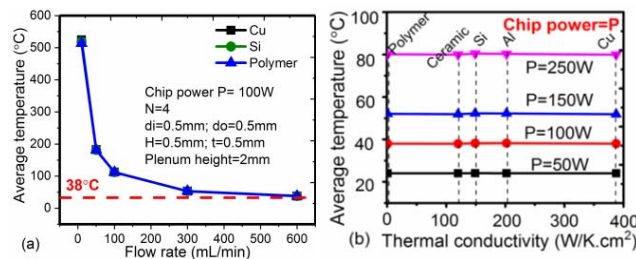


Figure 11. Modeling results for the impact of the cooler material on the chip temperature. A: Chip temperature as a function of flow rate for the different materials. B: Chip temperature as a function of cooler material thermal conductivity for different power levels.

From a thermal point of view, the coolant in the inlet plenum can be heated up at small flow rate due to the heat conduction between hotter outlet flow and the cold inlet flow. In order to study the impact on the chip temperature, the fluid and solid domain are both included in the CFD model shown in Fig.9. The fluid domain contains the inlet water domain and outlet water domain. Three different materials (Cu, Si and plastic) are studied when the flow rate increases from 50 ml/min to 600 ml/min. The temperature distribution across the cooler is shown in Fig.10. The simulations show that the impact of the cooler thermal conductivity on chip temperature distribution can be negligible over a wide range of flow rates and chip power, since the heat removal is dominated by the heat convection in the coolant. The trends summarized in Fig.11, show that a polymer cooler has the same performance as a Si or Cu cooler and therefore offers opportunities for the use of polymer based cost efficient fabrication techniques.

### D. Fabrication options for cooler designs

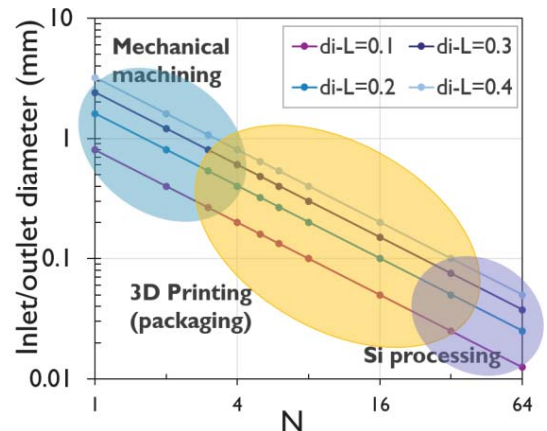


Figure 12. Link between the nozzle geometry and the fabrication technology options: mechanical machining process, 3D printing and Silicon processing

The choice of the number of nozzles and the nozzle diameter will have an impact on the required fabrication technology. Larger nozzle diameters will allow low cost fabrication techniques, while finer nozzle diameters require more expensive processing options. Fig.12 shows the link between inlet/outlet nozzle diameter and the nozzle number for the  $8 \times 8 \text{ mm}^2$  chip footprint and for different inlet diameter ratios  $d_i/L$ . In the chart, the applicable range is indicated for three fabrication technologies: mechanical machining, 3D printing and Si processing. Mechanical micro-machining especially micro-milling can be used to produce micro-features because it is simple and less time consuming. However, it is difficult to mill complex shape structures like cavity. Silicon processing has the advantage to fabricate small diameter holes below  $10 \mu\text{m}$  with Deep Reactive Ion Etching (DRIE) technology. However, the cost of silicon processing is higher than the other fabrication methods. Furthermore, the modeling study showed that aggressive scaling of the nozzle diameter is not required due to the saturation of the thermal performance. The required optimal diameter for the considered structures is in the order

of 100  $\mu\text{m}$  to several hundred  $\mu\text{m}$ . Thanks to the advancements in the recent years, 3D printing can be an interesting fabrication option to fabricate these structures with nozzle diameters ranging from 100  $\mu\text{m}$  to 1 mm. In the next section, an overview of the 3D printing technologies will be given.

### III. MANUFACTURABILITY OF 3D PRINTED COOLER

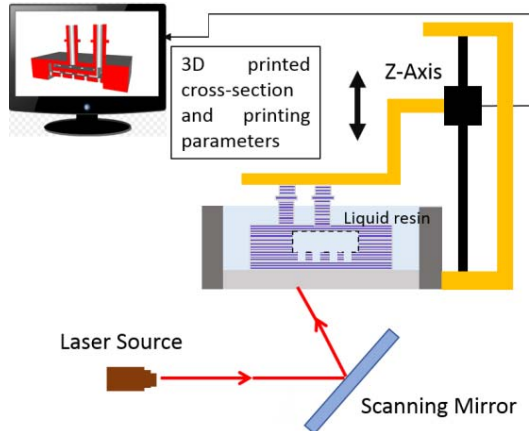


Figure 13. Principle of Stereo-lithography 3D printing

Fig.13 shows the principle of Stereo-lithography 3D printing technology. The cooler with complex structures is built in layers by focusing an ultraviolet (UV) laser on to a vat of photopolymer resin. Reported minimal feature size is 200  $\mu\text{m}$  for commercial tool of the supplier. In research tools, smaller feature sizes are possible since the resolution depends on the size of printing platform with fixed number of pixels.

#### A. State of art of 3D printing technology

Currently the highest resolution by 3D printing can be achieved through Two Photon Polymerization (TPP) process [12], which is one of 3D micro/nanoscale manufacturing technologies for arbitrary 3D structures with sub-100 nm resolution. Most of the materials used for TPP are designed for conventional lithographic applications, including negative and positive photoresist. However the TPP process is relative slow and small for this application. Alternatively, the Stereolithography (SL or SLA) process, which uses similar materials as the TPP but use either galvo scanners to guide the UV lasers or projector (when a projector is used the process is called DLP, or Digital Light Processing) to cure photopolymers layer by layer. The resolution could in micro meter range (for example 1 micron in Z direction (layer thickness) and a few to tens of microns in XY direction (pixel size). A comprehensive review of other micro Additive Manufacturing/3D printing technologies, such as SLM, Paste Extrusion, 3DP process etc., could be found in literature [12].

#### B. Critical parameters for the cooler design

In order to design a 3D printed cooler with sub-mm dimensions, two critical design parameters must be considered: 1) the nozzle wall thickness, which will make the separation between the inlet nozzle and the outlet plenum,

and 2) the nozzle diameter. For stereolithography and DLP, excess liquid resin needs to be removed from the internal cavities after curing of the polymer. This will form a constraint for designing nozzle diameters and plenum height in order to allow a successful draining of the excess resin. Therefore, the resin removal in the cooler design with small nozzle diameters and/or with limited plenum thickness is the major challenge for the use of additive manufacturing. The critical design parameters are visualized in Fig.14:

- the nozzle inlet and outlet diameters  $d_i$  and  $d_o$  and the gap  $S$  between two inlet nozzles can result in a resin removal issue due to the narrow gap;
- the nozzle side wall, with thickness  $W$ , should be sufficiently strong to prevent the wall from breaking, which can result in “short-circuit” between inlet flow and outlet flow;
- the plenum cavity thickness should be sufficient to support the structure, since a thin cavity wall can result in structure deformation.

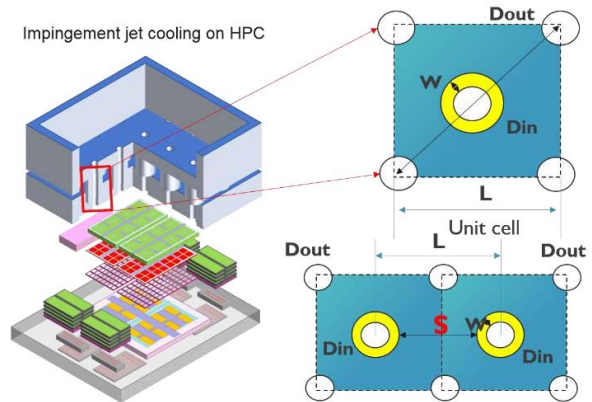


Figure 14. Visual representation of the critical design parameters for the use of 3D printing for impingement coolers.

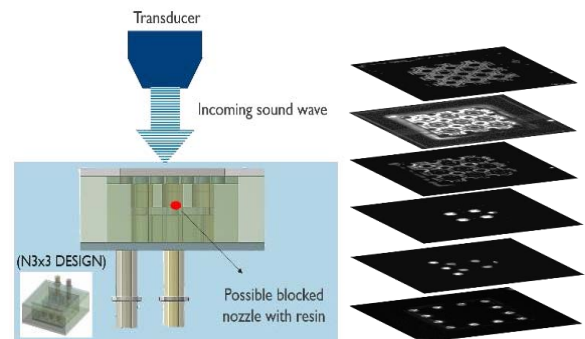


Figure 15. Illustration of the use of Scanning Acoustic Microscopy (SAM) to detect internal blockages in the 3D printed cooler at different depths.

Since the 3D printed cooler is printed as a single part, it is difficult to check for internal blockages with residual uncured resin. For this application, we demonstrated that the Scanning Acoustic Microscopy technique (SAM) can be used to evaluate the cooler quality. SAM is a non-destructive technique used for micro-inspection [13,14]. By adapting the focus depth, the potentially blocked resin inside the nozzles can be detected at different layers in the structure, as shown

in Fig.15. Fig. 16 shows an example of the SAM analysis of a printed cooler: from the SAM images it is possible to differentiate between the open nozzles without resin residues (A), open nozzles with tapered edges (B) and the presence of blocked nozzles (C).

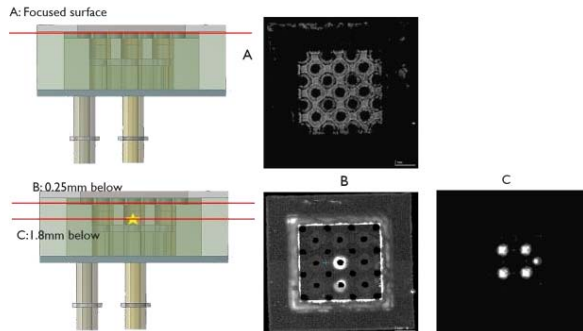


Figure 16. Results of the SAM analysis of a printed cooler with internal defects: open nozzles without resin residues (layer A), open nozzles with tapered edges (layer B), blocked nozzles (layer C).

#### IV. CHARACTERIZATION OF 3D PRINTED COOLER

In order to study the impact of the nozzle array scaling experimentally, different versions of the impingement cooler have been designed with a range of inlet nozzle numbers matching the  $8 \times 8$  mm<sup>2</sup> chip footprint. For this study, a commercial stereolithography technique (SLA) has been used, with a reported minimal feature size of 200  $\mu$ m, rather than the state of the art techniques described in the previous section. Taking into account the fabrication tolerance and the corresponding design limitations, the considered inlet nozzle arrays are  $3 \times 3$ ,  $4 \times 4$ ,  $6 \times 6$  and  $8 \times 8$ . For all the coolers, the same inlet diameter ratio  $d_i/L$  of 0.3 and the same ratio for the wall thickness are used, resulting in nozzle diameters ranging from 300 to 800  $\mu$ m. In this part, the impact of the printing tolerance on the fabricated structures and the thermal characterization of the printed coolers will be discussed.

##### A. Evaluation of the printed coolers

The top part of Fig.17 shows a cross-section of the design of the four coolers. For all the designs, the inlet/outlet diameter for the inlet/outlet tube is 2 mm, which will be connected with the outside tubing system. The inlet plenum height is about 2.5 mm, to allow the flow be uniformly distributed into every individual inlet nozzle. In order to guarantee that the strength is sufficiently high to withstand the high fluid pressure, the nozzle plate thickness should not be too thin. On the other hand, a thicker nozzle plate could generate more pressure drop inside the nozzle channel. In our design, the nozzle plate thickness is designed at 0.5 mm. Furthermore, the cavity height is designed at 0.6 mm to define the nozzle to chip distance since the impact of the cavity height can be neglected at the impingement jet region [3]. The dimensions for the scaled nozzle wall thickness and nozzle diameter of the four coolers are listed in Table 2.

The four coolers, fabricated using a water resistant polymer, are shown in the bottom part of Fig.17. The

photographs show a bottom view of the printed cooler, visualizing the nozzle plate with  $N \times N$  array of inlet nozzles and the distributed outlet nozzles in between. Visual inspection of the printed coolers reveals that all the nozzles are functional, and no trapped resin is observed for any of the four coolers, even for the cooler with the smallest features size that is very close to the reported printing capabilities. Since the inlet diameter is crucial for the cooler thermal performance, the fabrication accuracy of the four coolers is evaluated. The microscopy images of the inlet nozzles, shown in Fig.18, indicate that the fabricated nozzle diameter is about 0.15 mm larger than designed parameter for the  $3 \times 3$ ,  $4 \times 4$  and  $6 \times 6$  nozzle arrays. For the finest geometry of the  $8 \times 8$  nozzle array, the measured tolerance is about 0.08 mm. The designed and measured dimensions are compared in Table 1.

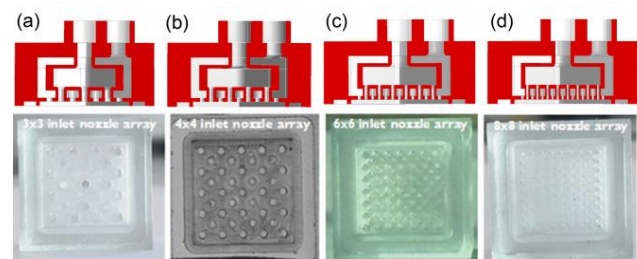


Figure 17. Design (top row) and photographs of the nozzle plates (bottom row) of the fabricated 3D printed coolers for the 4 cooler designs.

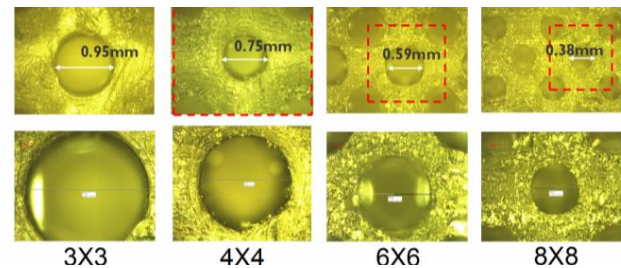


Figure 18. Diameter measurements of the inlet nozzles in the printed coolers. The red dashed box indicated the unit cell.

Table 1. Comparison between the designed and fabricated parameters (unit: mm)

$N \times N$ array	Unit cell	Wall thickness	$D_i$ -designed	$D_i$ -fabricated	New ratio
$3 \times 3$	2.67	0.4	0.8	0.95	0.36
$4 \times 4$	2	0.4	0.6	0.75	0.375
$6 \times 6$	1.33	0.25	0.4	0.59	0.44
$8 \times 8$	1	0.225	0.3	0.38	0.38

##### B. Thermal performance characterization

The printed coolers are all fully functional and have been successfully assembled to the bare die test chip packages that contain a  $8 \times 8$  mm<sup>2</sup> thermal test chip [15] with  $32 \times 32$  arrays of temperature sensors and 832 programmable heater cells. All four fabricated coolers have been characterized for a quasi-uniform power dissipation and a coolant flow rate ranging from 200 ml/min to 1000 ml/min. The measured averaged chip temperature is shown for the four coolers as a function of the flow rate in Fig. 19.

A very good thermal performance of  $0.13 \text{ cm}^2\text{-K/W}$  is observed for the  $8 \times 8$  cooler at  $1000 \text{ ml/min}$ . Furthermore, the measurement data can be used to assess the scaling trend for an increasing number of nozzles. The cooler with fewest nozzles ( $3 \times 3$ ) clearly has the lowest thermal performance, and the cooler with the highest number of nozzles has the best thermal performance ( $8 \times 8$ ). The results show however a similar result for the thermal resistance of the  $4 \times 4$  and  $6 \times 6$  design. This can be explained by the deviation of the fabricated nozzles from the designed geometry due to the printing accuracy. The fabricated nozzles are larger than the designed nozzle diameters. Therefore the fabricated coolers will have a higher thermal resistance than the designed coolers for the same flow rate, but require a lower pressure and lower pumping power.

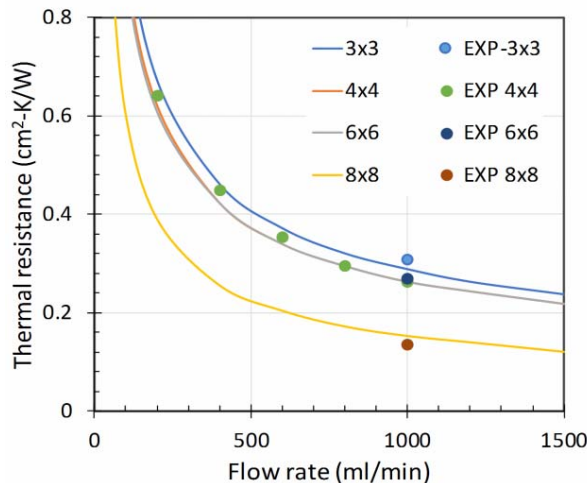


Figure 19. Experimental (markers) and modeling results (solid lines) of the cooler thermal resistance for the four fabricated coolers as a function of the coolant flow rate. The modeling results are obtained for the fabricated dimensions.

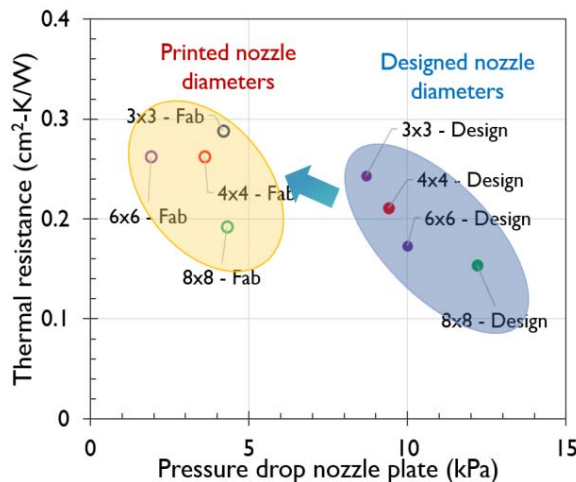


Figure 20. Modeling results for the impact of the printing tolerance on the thermal and hydraulic performance of the printed coolers for a coolant flow rate of  $1000 \text{ ml/min}$ .

Fig. 20 shows the comparison of the CFD modeling results for the designed and the fabricated nozzle diameters, indicating a similar performance for the fabricated  $4 \times 4$

$6 \times 6$  cooler. The updated nozzle ratios  $d/l$  based on the measurements have been added to Table 1. The thermal models have also been updated with the dimensions of the fabricated nozzles. These updated simulation results are shown as solid lines in Fig. 19 and show a very good agreement with the measurement data. The observed trend with increasing performance is:  $3 \times 3 < 4 \times 4 / 6 \times 6 < 8 \times 8$ .

## V. CONCLUSIONS

In this paper, we introduce 3D printing for the fabrication of a chip level polymer liquid jet impingement cooler, targeted to directly cool the backside of high performance chips or chip stacks. The modeling study shows that the thermal performance improves with an increasing inlet number of nozzles, but that a saturation of the performance is observed when the nozzle-to-target distance is kept constant. The optimal nozzle diameters obtained are in the order of  $100 \mu\text{m}$  to several hundred  $\mu\text{m}$ . Furthermore, the modeling results indicate that the thermal conductivity of the cooler material has no impact on the cooler performance. The required diameter dimensions and the opportunity to use polymers make 3D printing an attractive cost efficient option for the fabrication of the chip level coolers. It allows customization of the nozzle pattern design to match the heat map and the fabrication of complex internal structures. The main limitations of the considered stereolithography (SLA) technique are the limited feature size that can be fabricated and the need for the removal of the uncured excess resin from the cavities. We demonstrated that scanning acoustic microscopy (SAM) can be used to detect the presence of trapped resin.

Different versions of the impingement cooler have been designed with nozzle diameters ranging from  $300$  to  $800 \mu\text{m}$ . An optical inspection of the fabricated coolers showed that the printed nozzles are roughly  $150 \mu\text{m}$  wider than the designed diameter value. This results in a higher thermal resistance but a lower pressure drop in the cooler and lower required pumping power compared to the designed value. The cooler design with the finest nozzle diameters achieves a thermal resistance of  $0.13 \text{ cm}^2\text{-K/W}$  for a flow rate of  $1000 \text{ ml/min}$  and a low pressure drop. -

## ACKNOWLEDGMENT

This work was performed as part of the imec Industrial Affiliation Program on 3D System Integration and has been strongly supported by the imec partners and the imec Reliability, Electrical testing, Modeling and 3D technology teams. The authors would like to thank Ahmad Khaled for the SAM measurements.

## REFERENCES

- [1] T. Brunswiler *et al.*, "Benchmarking Study on the Thermal Management Landscape for Three-Dimensional Integrated Circuits: From Back-Side to Volumetric Heat Removal". ASME. J. Electron. Packag. 2016;138(1):010911-010911-10.
- [2] Tiwei Wei, *et al.*, "High efficiency direct liquid jet impingement cooling of high power devices using a 3D-shaped polymer cooler", IEDM, 2017.

- [3] T. Brunswiler *et al.*, "Direct Liquid Jet-Impringement Cooling with Micron-Sized Nozzle Array and Distributed Return Architecture", *proc. IEEE ITherm*, pp. 193-203, 2006.
- [4] Natarajan, G. and Bezama, R. J., "Microjet cooler with distributed returns," *Heat Transfer Eng.*, 28(8-9), pp.779–787, 2007.
- [5] Shariar Motakef, *et al.*, "Micro-Fabricated Solutions to Management of High Heat Flux Systems", *CoolingZone's Online Magazine*, June, 2005.
- [6] G. Aspar, *et al.*, "3D Printing as a New Packaging Approach for MEMS and Electronic Devices", 2017 IEEE 67th Electronic Components and Technology Conference (ECTC), pp.1071-1079.
- [7] Michael Craton, *et al.*, "3D Printed High Frequency Coaxial Transmission Line Based Circuits", 2017 IEEE 67th Electronic Components and Technology Conference (ECTC), pp.1080-1087.
- [8] Xing Lan, *et al.*, "3-D Inkjet Printed Ultra-Wideband Equi-Angular Spiral Antennas", 2016 IEEE 67th Electronic Components and Technology Conference (ECTC), pp.823-828.
- [9] Tobias Tiedje, *et al.*, "Will Low-Cost 3D Additive Manufactured Packaging Replace the Fan-Out Wafer Level Packages?", 2017 ECTC, pp.1065-1070.
- [10] C Bailey, *et al.*, "3D-printing and electronic packaging", *Pan Pacific Microelectronics Symposium (Pan Pacific)*, 2016.
- [11] Tiwei Wei, H. Oprins, *et al.*, "Nozzle array scaling effects on the thermal/hydraulic performance of liquid jet impingement coolers for high performance electrnc applications", *IHTC 2018*.
- [12] Vaezi, M.; Seitz, H.; Yang, S. F., A review on 3D micro-additive manufacturing technologies. *Int J Adv Manuf Tech* 2013, 67, (5-8), 1721-1754.
- [13] Janting J. "Techniques in Scanning Acoustic Microscopy for Enhanced Failure and Material Analysis of Microsystems". In: Leondes C.T. (eds) *MEMS/NEMS*. Springer, Boston, MA, 2006.
- [14] Khaled, A. *et al.*, "Investigating stress measurement capabilities using GHz scanning acoustic microscopy for 3D failure analysis", *Microelectronics Reliability*. Vol. 64: 336-340; 2016.
- [15] H. Oprins *et al.*, "Experimental characterization of the vertical and lateral heat transfer in three-dimensional stacked die packages", *J. Electron. Packaging*, vol. 138, pp. 101902 1-10, 2016.